Radiation Measurements 58 (2013) 12–17

Contents lists available at ScienceDirect

Radiation Measurements

journal homepage: www.elsevier.com/locate/radmeas

A comparison of different discrimination parameters for the DFT-based PSD method in fast scintillators

G. Liu*, J. Yang, X.L. Luo, C.B. Lin, J.X. Peng, Y. Yang

Department of Instrument Science and Technology, National University of Defense Technology, Changsha 410073, China

HIGHLIGHTS

- The spectrum difference between neutron pulse and γ-ray pulse was investigated.
- The DFT-based PSD with different parameter definitions was assessed.
- The way of using the ratio of magnitude spectrum provides the best performance.
- The performance differences were explained from noise suppression features.

ARTICLE INFO

Article history:
Received 30 April 2012
Received in revised form
5 April 2013
Accepted 22 July 2013

Keywords:
DFT-based PSD
Discrimination parameter
Digital discrimination
Liquid scintillator

ABSTRACT

Although the discrete Fourier transform (DFT) based pulse shape discrimination (PSD) method, realized by transforming the digitized scintillation pulses into frequency coefficients by using DFT, has been proven to effectively discriminate neutrons and γ rays, its discrimination performance depends strongly on the selection of the discrimination parameter obtained by the combination of these frequency coefficients. In order to thoroughly understand and apply the DFT-based PSD in organic scintillation detectors, a comparison of three different discrimination parameters, i.e. the amplitude of zero-frequency component, the amplitude difference between the amplitude of zero-frequency component and the amplitude of base-frequency component, and the ratio of the amplitude of base-frequency component to the amplitude of zero-frequency component, is described in this paper. An experimental setup consisting of an Americium–Beryllium (Am–Be) source, a BC501A liquid scintillator detector, and a 5Gsample/s 8-bit oscilloscope was built to assess the performance of the DFT-based PSD with each of these discrimination parameters in terms of the figure-of-merit (based on the separation of the event distributions). The third technique, which uses the ratio of the amplitude of base-frequency component to the amplitude of zero-frequency component as the discrimination parameter, is observed to provide the best discrimination performance in this research.

1. Introduction

Organic scintillation detectors have often been used for the detection and spectroscopy of a wide assortment of radiations. When they are used as neutron detectors, pulse shape discrimination (PSD) is an essential requirement because all neutron fields coexist with an associated γ-ray component, arising as a result of scattering reactions of the neutrons with materials in the environment and as direct by-products of the primary reaction producing the neutron field (Knoll, 2000). Besides, by applying the n/γ PSD technique, it is possible to measure the spectra of neutrons and γ rays concurrently in a single measurement.

More recently, a number of techniques for PSD have been implemented in the digital domain as digital electronic platforms have become available with the requisite speed and cost. According to the characteristics of the separation parameters, these discrimination methods can be classified as a time domain PSD and frequency domain PSD (Saleh et al., 2012). The time domain PSD, such as the zero crossing method (Nakhostin and Walker, 2010), the charge comparison method (Ambers et al., 2011), the correlation method (Kornilov et al., 2003), the curve-fitting method (Marrone et al., 2002) and the method of pulse gradient analysis (PGA) (D′ Mellow et al., 2007), can usually provide real-time, digital characterization of environments where neutrons and γ rays coexist. But because the time domain features are naturally highly

* Corresponding author. Tel.: +86 731 84573383; fax: +86 731 84574962.
E-mail addresses: lgflh@163.com, guofu.liu@nudt.edu.cn (G. Liu).

1350-4487/$ – see front matter © 2013 Elsevier Ltd. All rights reserved.
http://dx.doi.org/10.1016/j.radmeas.2013.07.008

dependent on the signal amplitude at specific times, these methods based on time domain features are sensitive to the natural variance and noise in the pulse response arising from the photomultiplier tube (PMT) and the measurement circuit, and therefore the discrimination performance has a great dependency on the de-noising algorithm. The frequency domain PSD, obtained by transforming the digitized scintillation pulses into frequency coefficients by using any frequency transform, such as Discrete Fourier Transform (DFT) or Discrete Wavelet Transform (DWT), is more robust to the variance and noise in the detection system and therefore does a better discrimination than the time domain PSD (Liu et al., 2010; Arafa et al., 6–7 APRIL, 2009; Yousefi et al., 2009; Shippen et al., 2010). For the DWT-based PSD is usually highly computationally intensive and hence not suitable for real-time field measurements, more and more attention has been given to the DFT-based PSD.

In order to combine the advantage of insensitivity to pulse variation and noise associated with spectral analysis with that of real-time implementation, generally only the first two components of DFT, i.e. the zero-frequency component and the base-frequency component, have been calculated. It is obvious that the method of defining the discrimination parameter from these two components has a great effect on the performance of the DFT-based PSD. In this work, we described the comparison of figure-of-merits (based on the separation of the event distributions) determined with three different discrimination parameters for the DFT-based PSD method on events from a fast scintillation detector.

This paper is organized as follows: first, the principle of DFT-based PSD and three definitions of discrimination parameters are described in Section 2. Second, a detailed description of the experimental environment is given in Section 3. The results and discussion are given in Section 4. Finally, Section 5 concludes this paper.

2. The principle of DFT-based PSD with different discrimination parameters

2.1. The principle of DFT-based PSD

Assuming that the digitalized scintillation pulse signal is $x(n)(n = 0,1,...N-1)$, its discrete Fourier transform (DFT) $X(k)$ can be obtained through the following analysis equation (Oppenheim et al., 1999)

$$X(k) = \sum_{n=0}^{N-1} x(n)\exp\left(-\mathrm{j}\frac{2\pi}{N}nk\right) \quad k = 0,1,...,N-1 \tag{1}$$

where the integer variable n is the discrete time index, N is the sample length, and the integer index k represents the discrete frequency variable, which corresponds to an actual frequency of $2k\pi/N$ rad/s or kF_s/N Hz where F_s is the sampling frequency in units of Hz. According to Eq. (1), we also can obtain the magnitude spectrum $|X(k)|$ and the power spectrum $|X(k)|^2/N$ of the digitalized scintillation pulse signal, respectively.

A typical pulse shape according to the six parameter function of Marrone's model (Marrone et al., 2002; Liu et al., 2010) for each radiation type is given in Fig. 1. It is clearly shown that the neutron-induced pulse decays more slowly than the pulse stimulated by γ ray, because neutrons show great energy loss rate during their interaction than γ rays.

The corresponding magnitude spectrum of each radiation type is calculated by using Eq. (1). The results show that there is little difference between the magnitude spectrum of neutron-induced pulse and that of γ-ray pulse at higher frequency, and hence only some lower frequency components of DFT are given in Fig. 2. It can

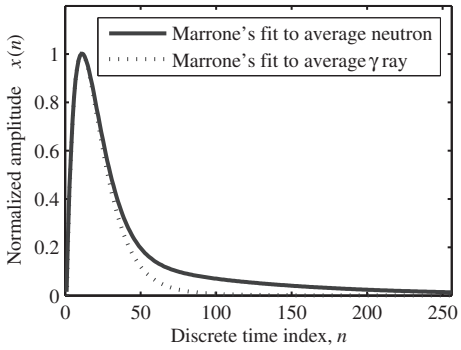

Fig. 1. A plot of normalized amplitude versus discrete time index for an average neutron (solid line) and γ-ray pulse shape (dot line).

be clearly seen from Fig. 2 that at $k = 0$, i.e. at zero-frequency, there is a distinct difference between the magnitude spectrum of neutron pulse and that of γ-ray pulse, which can be used as a prominent feature to discriminate neutrons and γ rays.

2.2. Three definitions of discrimination parameters of DFT-based PSD

Exploiting this feature and considering the requirement of real implementation, three typical definitions of discrimination parameters have been proposed as follows.

(1) The first method of defining the discrimination parameter, which directly uses the feature that $|X(0)|$ of neutron pulse is much bigger than that of γ-ray pulse, is described as

$$d_{11} = \frac{1}{N}|X(0)| \text{ or } d_{12} = \frac{1}{N}|X(0)|^2 \tag{2}$$

(2) The second method of defining the discrimination parameter, which is proposed by G. Liu et al. (Liu et al., 2010), is described as

$$d_{21} = \frac{1}{N}(|X(0)| - |X(1)|) \text{ or } d_{22} = \frac{1}{N}\left(|X(0)|^2 - |X(1)|^2\right) \tag{3}$$

(3) The third method of defining the discrimination parameter, which is proposed by Arafa et al., 6–7 APRIL (2009), is described as

$$d_{31} = 1 - \frac{|X(1)|}{|X(0)|} \text{ or } d_{32} = 1 - \frac{|X(1)|^2}{|X(0)|^2} \tag{4}$$

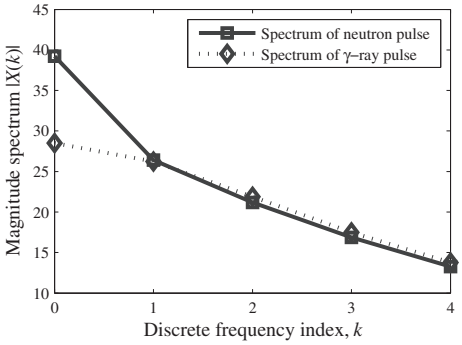

Fig. 2. The lower frequency components of the magnitude spectrum of the average neutron pulse (solid line) and that of the average γ-ray pulse (dot line).

In the above equations, $d_{ij}(i = 1,2,3; j = 1,2)$ represents different discrimination parameter, the subscript i indicates one of the methods, and j indicates the method of using the magnitude spectrum or power spectrum.

According to the above definitions, for only the first two frequency components of DFT, i.e. the zero-frequency component and the base-frequency component, need to be calculated to obtain the discrimination parameter, it is not necessary to calculate the amplitudes of all the frequency components of DFT. $|X(0)|$ and $|X(1)|$ can be calculated by using the following equations

$$\begin{cases} |X(0)| = \left| \sum_{n=0}^{N-1} x(n) \right| \\ |X(1)| = \sqrt{\left(\sum_{n=0}^{N-1} x(n) \cos \frac{2\pi n}{N} \right)^2 + \left(\sum_{n=0}^{N-1} x(n) \sin \frac{2\pi n}{N} \right)^2} \end{cases} \tag{5}$$

If the values of $cos(2\pi n/N)$ and $\sin(2\pi n/N)$ are calculated in advance, $|X(1)|$ can be obtained quickly with a lookup table.

In order to investigate the effects of these different definitions of discriminator parameters on the performance of DFT-based PSD, we will compare the figure-of-merits (based on the separation of the event distributions) determined with these definitions for DFT-based PSD on events from a fast scintillation detector.

3. Experimental methods

The experimental data analyzed in this work were acquired using a radiation measurement system at the Institute of Nuclear Physics and Chemistry, the Chinese Academy of Engineering Physics, Mianyang, China. The experimental arrangement is shown schematically in Fig. 3. A BC501A organic liquid scintillator was exposed to a mixed radiation fields produced by a ^{241}Am–Be radioisotope neutron source suspended on a three-legged stand. The neutron source was positioned 1750 mm away from the ground of the laboratory and with a distance of 1150 mm to the scintillation detector at the same height. The liquid scintillation detector consisted of a Φ50.8 mm × 50.8 mm cylindrical cell scintillation detector filled with BC501A organic liquid, optically-coupled to an EMI 9807B photomultiplier tube (PMT), which was operated with a negative supply voltage of −1400 V DC. The output signal from the liquid scintillator was connected to channel 1 of a Tektronix digital phosphor oscilloscope, via approximately 25 m of the high bandwidth cable. The liquid scintillator pulse

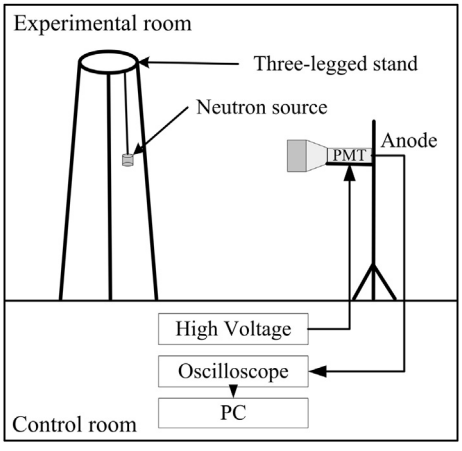

Fig. 3. A schematic diagram of the experimental set-up at the Chinese Academy of Engineering Physics. The location of the source, detector and cables are not to scale.

data were captured digitally by the oscilloscope with a sampling rate of 2.5GSa/s and 8-bit amplitude resolution which were then streamed to a PC over a USB connection using USB2.0 protocol. Each pulse shape consisted of 1000 samples taken at 0.4 ns intervals, and approximately 10,000 digitized events were collected.

4. Results and discussion

According to the total yields of neutrons and γ-rays of the Am–Be neutron source, the geometric structure and the relative position of the neutron source and the detector, the estimated count rate is about 127/s. The probability for pile-up of the signals is very small. Therefore the effect of pile-up on the discrimination performance will be negligible in the following calculations and discussions.

4.1. Discrimination results of DFT-based PSD with different discrimination parameters

According to the principle of the DFT-based PSD method described in Section 2, the scatter plots of peak amplitude against different discrimination parameters are shown in Fig. 4. The total number of events is 8964 used for discrimination. As explained in Section 2, we know that a neutron-induced pulse has a higher discrimination value for the same peak amplitude than that of a γ ray. Hence, two plumes are evidently separated in terms of discrimination parameter relative to peak amplitude, which correspond to γ-ray and neutron events. The neutrons correspond to the events in the right plume whereas the γ rays correspond to the events in the left plume in the plots.

4.2. Comparison of discrimination performances of DFT-based PSD with different discrimination parameters

To evaluate the separation of the neutron and γ-ray plumes and to compare the discrimination performances of the DFT-based PSD with different discrimination parameters, the corresponding probability distribution histograms with fitted Gaussian distributions are given in Fig. 5.

The corresponding figure-of-merit (FOM) values for each discrimination parameter have also been calculated using Eq. (6):

$$\mathrm{FOM} = \frac{S}{\mathrm{FWHM}_\gamma + \mathrm{FWHM}_n} \tag{6}$$

where S is the separation between the centroids of the neutron peak and the γ-ray peak in the spectrum, FWHM_γ is the full-width-half-maximum(FWHM)of the spread of events classified as γ-ray events and FWHM_n is the FWHM of the spread in the neutron peak (Winyard et al., 1971). If the probability distribution function of each event is consistent with Gaussian distribution, Eq. (6) becomes

$$\mathrm{FOM} = \frac{|\mu_\mathrm{n} - \mu_\gamma|}{2.35(\sigma_\gamma + \sigma_n)} \tag{7}$$

where μ_γ and μ_n are the means of the γ-ray and neutron Gaussians, respectively. The standard deviation, σ, is given as σ_γ and σ_n for the γ-ray and neutron Gaussians. The values of these parameters and the corresponding FOMs under different discrimination parameters from the experimental results shown in Fig. 5 are tabulated in Table 1.

4.3. Discussion

According to Figs. 4 and 5 and Table 1, it is clearly shown that the DFT-based PSD method with the third definition of discrimination parameter, i.e. d_{31} or d_{32}, has the highest FOM, whereas the method with the first definition, i.e. d_{11} or d_{12}, has the lowest FOM.

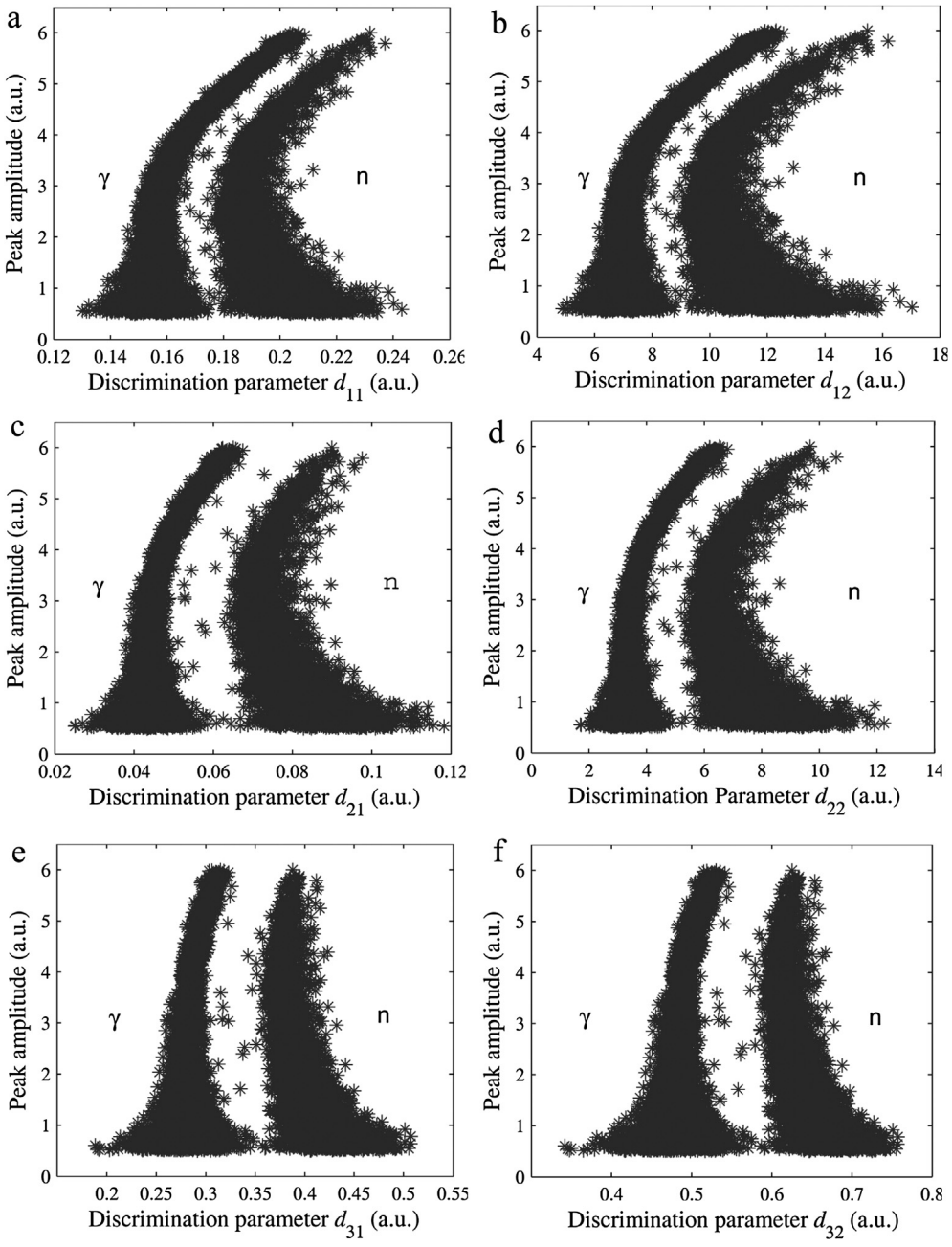

Fig. 4. Scatter plots of peak amplitude versus each discrimination parameter defined by Eqs. (2)–(4). (a) d_{11}, (b) d_{12}, (c) d_{21}, (d) d_{22}, (e) d_{31}, (f) d_{32}. The trigger threshold value is approximately 0.5, corresponding to the light output of approximately 350 keV of electron-equivalent recoil energy (keVee).

The difference of their performances may be explained qualitatively from their corresponding noise suppression features as follows.

Assuming that the digitalized scintillation pulse signal $x(n)$ is modeled as the sum of the standard pulse shape $s(n)$ and the noise noise(n), we have

$$x(n) = s(n) + \text{noise}(n) \quad n = 0, 1, ..., N-1 \tag{8}$$

Here, $s(n)$ can be obtained by averaging a number of signal pulses of the same particles (Marrone et al., 2002), and noise(n)

Table 1
The values of parameters in Eq. (7) calculated from the experimental results shown in Fig. 5 and the corresponding FOMs under different discrimination parameters.

d	μ_γ	σ_γ	μ_n	σ_n	FOM
d_{11}	0.1558 ± 0.0003	0.0057 ± 0.0003	0.1926 ± 0.0004	0.0100 ± 0.0004	0.9975 ± 0.0345
d_{12}	6.999 ± 0.021	0.5040 ± 0.0216	10.69 ± 0.04	1.100 ± 0.043	0.9792 ± 0.0317
d_{21}	0.0439 ± 0.0003	0.0038 ± 0.0003	0.0763 ± 0.0004	0.0087 ± 0.0004	1.103 ± 0.047
d_{22}	3.395 ± 0.017	0.3636 ± 0.0174	6.716 ± 0.055	1.037 ± 0.055	1.009 ± 0.045
d_{31}	0.2830 ± 0.0010	0.0150 ± 0.0009	0.3955 ± 0.0018	0.0245 ± 0.0010	1.212 ± 0.046
d_{32}	0.4873 ± 0.0014	0.0211 ± 0.0010	0.6355 ± 0.0021	0.0298 ± 0.0015	1.237 ± 0.048

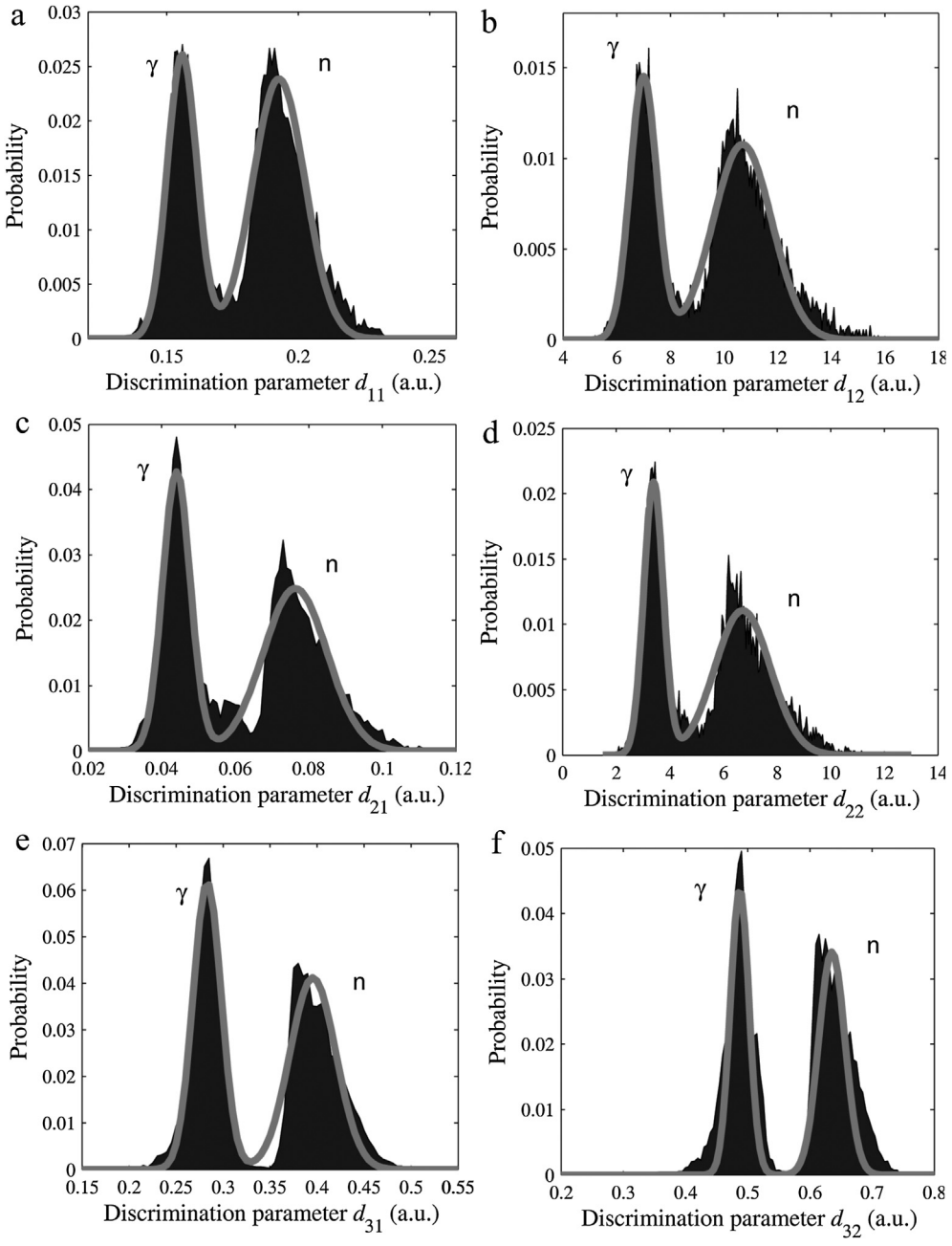

Fig. 5. The corresponding probability distribution histograms with fitted Gaussian distributions for the data shown in Fig. 4. (a) d_{11}, (b) d_{12}, (c) d_{21}, (d) d_{22}, (e) d_{31}, (f) d_{32}.

is the total summation of effects of the photons statistics, the phototube response and the electronics noise. In the frequency domain, the noisy signal Eq. (8) can be expressed as

$$X(k) = S(k) + N(k) \quad k = 0, 1, ..., N-1 \tag{9}$$

where the complex variable $X(k)$, $S(k)$ and $N(k)$ are the discrete Fourier transform (DFT) of $x(n)$, $s(n)$ and noise(n) respectively. Substitute Eq. (9) into Eqs. (2)–(4), respectively, we have

$$\begin{cases} d_{11} = \frac{1}{N}|X(0)| = \frac{1}{N}|S(0) + N(0)| \\ d_{12} = \frac{1}{N}|X(0)|^2 = \frac{1}{N}\left(S^2\left(0\right) + N^2\left(0\right)\right) \end{cases} \tag{10}$$

$$\begin{cases} d_{21} = \frac{1}{N}\left(|X(0)| - |X(1)|\right) = \frac{1}{N}\left(|S(0) + N(0)| - |S(1) + N(1)|\right) \\ d_{22} = \frac{1}{N}\left(|X(0)|^2 - |X(1)|^2\right) = \frac{1}{N}\left(\left(S^2\left(0\right) - S^2\left(1\right)\right) + \left(N^2\left(0\right) - N^2\left(1\right)\right)\right) \end{cases} \tag{11}$$

$$\begin{cases} d_{31} = 1 - \frac{|X(1)|}{|X(0)|} = 1 - \frac{|S(1)+N(1)|}{|S(0)+N(0)|} \\ d_{32} = 1 - \frac{|X(1)|^2}{|X(0)|^2} = 1 - \frac{S^2(1)+N^2(1)}{S^2(0)+N^2(0)} \end{cases} \quad (12)$$

In the above equations, we assume that the standard pulse signal and the noise processes are uncorrelated ergodic processes. According to these equations, we can qualitatively illuminate the discrimination performances of the DFT-based PSD method with different definitions of discrimination parameters. In Eq. (10), the noise spectrum is directly superimposed on the spectrum of the standard pulse resulting in a strong fluctuation of d_{11} and d_{12}. While in Eq. (11), d_{21} and d_{22} are calculated by the process of spectral subtraction, which suppresses the influence of noise on the discrimination performance intensively. Further in Eq. (12), d_{31} and d_{32} are defined by the process of spectral subtraction normalized by the magnitude of the spectrum of zero-frequency component, which lowers the dependency of the discrimination parameter on the peak amplitude.

It is worth noting that the second and third definitions have also lowered the effects of some non-stationary noises, such as 1/f noise, impulsive noise and transient noise existed in the scintillation detection system provided that their power spectral do not change abruptly.

5. Conclusions

A comparison of different discrimination parameters for the DFT-based PSD method in fast scintillators has been investigated theoretically and experimentally in detail. First, the general principle of DFT-based PSD method to discriminate neutrons and γ rays was analyzed, i.e. there is a distinct difference between the magnitude spectrum of neutron pulse and that of γ-ray pulse, which can be used as a prominent feature to discriminate neutrons and γ rays. By exploiting this feature and considering the requirement of real implementation, three typical definitions of discrimination parameters have been proposed. Second, an experimental system comprising of a ^{241}Am–Be radioisotope neutron source, a BC501A liquid scintillator and a 5Gsample/s 8-bit oscilloscope was built to assess the performance of the DFT-based PSD with each of these discrimination parameters in terms of the figure-of-merit (based on the separation of the event distributions). Finally, the experiment data were processed and the results showed that the DFT-based PSD method with the third definition of discrimination parameter, i.e. d_{31} or d_{32}, has the highest FOM, whereas the method with the first definition, i.e. d_{11} or d_{12}, has the lowest FOM. The difference of their performances has been explained qualitatively from their corresponding noise suppression features.

Acknowledgments

We acknowledge the support of the Institute of Nuclear Physics and Chemistry, the Chinese Academy of Engineering Physics, Mianyang, China. We gratefully acknowledge the help and advice of Dr. Li An and Dr. Pu Zheng and the technical team at the Chinese Academy of Engineering Physics, Mianyang, China. This work was supported by the Natural Science Foundation of China (NSFC) Grant #11175254. Its contents are solely the responsibility of the authors and do not necessarily represent the official views of the NSFC.

References

Ambers, S.D., Flaska, M., Pozzi, S.A., 2011. Nucl. Instr. Meth. A 638, 116–121.
Arafa, A., Saleh, H., Ashour, M., Salem, A., 6–7 APRIL 2009. Fourth IEEE International Conference on Design &Technology of Integrated Systems in Nanoscale Era, p. DTIS09.
D' Mellow, B., Aspinall, M.D., Mackin, R.O., Joyce, M.J., Peyton, A.J., 2007. Nucl. Instr. Meth. A 578, 191–197.
Knoll, G.F., 2000. Radiation Detection and Measurement, third ed. Wiley, New York.
Kornilov, N.V., Khriatchkov, V.A., Dunaev, M., Kagalenko, A.B., Semenova, N.N., Demenkov, V.G., Plompen, A.J.M., 2003. Nucl. Instr. Meth. A 497, 467–478.
Liu, G., Joyce, M.J., Ma, X., Aspinall, M.D., 2010. IEEE Trans. Nucl. Sci., 1682–1691. NS-57.
Marrone, S., Cano-Ott, D., Colonna, N., Domingo, C., Gramegna, F., Gonzalez, E.M., Gunsing, F., Heil, M., Kappeler, F., Mastinu, P.F., et al., 2002. Nucl. Instr. Meth. A 490, 299–307.
Nakhostin, M., Walker, P.M., 2010. Nucl. Instr. Meth. A 621, 498–501.
Oppenheim, A.V., Schafer, R.W., Buck, J.R., 1999. Discrete-time Signal Processing, second ed. Prentice-Hall.
Saleh, H., Yahya, A., Sayed, M., Ashour, M., 2012. Int. J. Comput. Appl. 38, 6–12.
Shippen, D.I., Joyce, M.J., Aspinall, M.D., 2010. IEEE Trans. Nucl. Sci., 2617–2625. NS-57.
Winyard, R.A., Lukin, J.E., McBeth, B.W., 1971. Nucl. Instr. Meth. 95, 141–153.
Yousefi, S., Lucchese, L., Aspinall, M.D., 2009. Nucl. Instr. Meth. A 598, 551–555.